# Observed Associations Among Storm Tracks, Jet Streams and Midlatitude Oceanic Fronts

Hisashi Nakamura[1],[2], Takeaki Sampe[1], Youichi Tanimoto[2],[3], and Akihiko Shimpo[4]

An association is discussed among a midlatitude storm track, a westerly polar-front jet stream and an underlying oceanic frontal zone. Their close association is observed when a subtropical jet stream is weak, as in the Southern Hemisphere summer or in the North Atlantic. Along a near-surface baroclinic zone that tends to be anchored around a frontal zone, storm track activity is enhanced within a well-defined polar-front jet with modest core velocity. This eddy-driven jet exhibits a deep structure with the strong surface westerlies maintained mainly through a poleward eddy heat flux. The westerly wind stress exerted along the frontal zone acts to maintain it by driving the oceanic current system, suggestive of a feedback loop via midlatitude atmosphere–ocean interaction. It is argued that the context of this feedback must be included in interpreting the tropospheric general circulation and its variability. In fact, decadal-scale sea–surface temperature anomalies observed in the North Pacific subarctic frontal zone controlled the anomalous heat release to the atmosphere. Seemingly, the local storm track responded consistently to the decadal-scale shift of the frontal axis, acting to reinforce basin-scale flow anomalies. Over the North and South Pacific, the association is disturbed in winter by an intensified subtropical jet that traps eddy activity into its sharp core. The trapping impairs baroclinic interaction of upper-level eddies with the surface baroclinicity along a midlatitude oceanic front, leading to the suppression of eddy activity as observed in midwinter over the North Pacific.

## 1. INTRODUCTION

Synoptic-scale baroclinic eddies migrating along mid-latitude storm tracks not only influence daily weather but also play a crucial role in the climate system by systematically transporting heat, moisture and angular momentum. Seasonal variations of synoptic-scale eddies have been examined for the Northern Hemisphere (NH) [*Petterssen*, 1956; *Klein,* 1958; *Whittaker and Horn,* 1984; *Rogers,* 1990] and the Southern Hemisphere (SH) [*Sinclair,* 1994, 1995; *Simmonds and Keay,* 2000], by tracking the centers of individual moving cyclones (or anticyclones) at the surface. The "Lagrangian-type" approach based on cyclone tracks ("storm tracks" in this framework) is a straightforward application of weather chart analysis. *Hoskins and Hodges* [2002] applied this tracking method to upper-level fields of other variables from which planetary-scale signals had been removed.

In addition to the "synoptic" viewpoint, another approach has been adopted, where emphasis is placed on propagation behavior of wavy disturbances and their ensemble feedback on

[1]Department of Earth and Planetary Science, University of Tokyo, Tokyo, Japan.
[2]Frontier Research System for Global Change, Yokohama, Japan.
[3]Graduate School of Environmental Earth Science, Hokkaido University, Sapporo, Japan.
[4]Climate Prediction Division, Marine and Climate Department, Japan Meteorological Agency, Tokyo, Japan.

The Earth's Climate: The Ocean-Atmosphere Interaction
Geophysical Monograph 147, pp. 329-346

10.1029/147GM18

the time-mean flow in which they are embedded. This "Eulerian-type" approach is based on high-pass filtering of daily time series at individual grid points, for extracting subweekly fluctuations associated with migratory synoptic-scale eddies [*Blackmon et al.,* 1977, 1984]. In this "wave dynamic" approach, regions of large variance in geopotential height or meridional wind velocity or of a strong poleward eddy heat flux are called "storm tracks", and "storm track activity" signifies the magnitude of the variance or heat flux. *Wallace et al.* [1988] discussed the relationship between cyclone and anticyclone tracks in the synoptic framework and storm tracks in the wave dynamic viewpoint. Though critically argued recently [*Held,* 1999], this approach has an advantage that local correlation between high-pass-filtered time series of air temperature and meridional wind velocity or vertical motion gives a measure for baroclinic structure of migratory eddies. The high positive correlation indicates baroclinic structure of those eddies that allows efficient energy conversion from the time-mean flow for their growth. Climatological seasonal variations observed in storm tracks were documented in this framework by *Trenberth* [1991] and *Nakamura and Shimpo* [2004, hereafter *NS04*] for the SH and by *Nakamura* [1992, hereafter *N92*] for the NH. Some of the related dynamical issues are discussed by *Cai* [2004].

As reviewed by *Chang et al.* [2002], recent studies have substantiated a notion of downstream development, in recognition of group-velocity propagation of synoptic eddies along storm tracks [*Chang,* 1993, 1999; *Lee and Held,* 1993; *Swanson and Pierrehumbert,* 1994; *Orlanski and Chang,* 1995; *Berbery and Vera*, 1996; *Chang and Yu*, 1999; *Rao et al.,* 2002]. The notion requires us to interpret eddy statistics in relation to cyclogenesis from a viewpoint of an initial value problem. This type of cyclogenesis has been known as the "B-type cyclogenesis" [*Petterssen and Smebye,* 1971] or "coupling development" [*Takayabu,* 1991], to which *Hoskins et al.* [1985] added further elucidation from a potential-vorticity (PV) perspective. In the "PV thinking", baroclinic eddy growth is interpreted as mutual reinforcement between PV anomalies at the tropopause and those in the form of temperature anomalies at the surface. In the downstream development, the thermal anomalies are triggered by wind fluctuations across a surface baroclinic zone induced by a propagating upper-level vortex. Thus, surface temperature gradient is of particular significance in baroclinic instability. Nevertheless, in most of the studies from the wave dynamic perspective, storm tracks have been regarded as a pure atmospheric issue.

Forecast experiments have shown the importance of heat and moisture supply from the warm ocean surface of the Gulf Stream or Kuroshio in individual events of rapid cyclone development [*Nuss and Kamikawa,* 1990; *Kuo et al.,* 1991; *Reed et al.,* 1993; *Neiman and Shapiro*, 1993]. A regional-model experiment by *Xie et al.* [2002] indicates that cyclone development is sensitive to a fine frontal structure in a sea–surface temperature (SST) field between the Kuroshio and the shallow East China Sea. Climatologically, rapid cyclone development over the NH is most likely along the Gulf Stream and Kuroshio [*Sanders and Gyakum,* 1980]. Over the SH, maritime cyclogenesis is most frequent around an intense oceanic frontal zone in the Indian Ocean [*Sinclair*, 1995]. These observational tendencies suggest the oceanic influence on storm track formation. At the same time, storm tracks can in turn influence the underlying ocean. By means mainly of their poleward heat flux, eddies migrating along a storm track transfer the mean-flow westerly momentum downward, acting to sustain the surface westerlies [*Lau and Holopainen,* 1984]. In fact, *Hoskins and Valdes* [1990, hereafter *HV90*] considered a storm track could be self-maintained under the heat and moisture supply from a nearby warm ocean current that is driven by the eddy-maintained surface westerlies. Those eddies also supply fresh water to the ocean along the storm track, influencing the stratification in the midlatitude upper ocean [*Lukas,* 2001].

The main purpose of this paper is to further discuss the importance of the atmosphere–ocean coupling via storm tracks in the tropospheric circulation system and its long-term variability from the wave dynamic viewpoint, based on observational statistics. Our argument may be viewed as an extension of *HV90*, but unlike in *HV90*, we put emphasis on oceanic frontal zones associated with major oceanic currents. As the surface air temperature over the open ocean is linked to SST underneath, maritime surface baroclinic zones tend to be anchored along oceanic fontal zones [*NS04*]. Though acting as thermal damping for the evolution of individual eddies, heat exchange with the underlying ocean, on longer time scales, can act to restore atmospheric near-surface baroclinicity against the relaxing effect by atmospheric eddy heat transport, as evident in sharp meridional contrasts in upward turbulent heat fluxes observed climatologically across midlatitude frontal zones [*Oberhuber,* 1988]. Some observations are shown in section 2 to suggest that SST anomalies in a midlatitude frontal zone can likely play a more active role in the air–sea interaction than act to damp atmospheric anomalies thermally. In section 3, we discuss associations among storm tracks, polar–frontal (or subpolar) jet streams and underlying oceanic frontal zones over the two hemispheres. In section 4, we then discuss how such an association can be disturbed in winter by the intensification of a subtropical jet stream. In the final section, we propose a working hypothesis through which our understanding might be deepened on the observed tropospheric circulation system and its variability.

## 2. IMPORTANCE OF STORM TRACKS AND OCEANIC FRONTAL ZONES IN EXTRATROPICAL COUPLED OCEAN–ATMOSPHERE VARIABILITY

### *2.1. Atmospheric Forcing Over Central/Eastern Basins*

The interaction between the midlatitude ocean and storm tracks is by no means a new concept. The importance has been emphasized in the notion of the "atmospheric bridge", through which the effect of tropical Pacific SST anomalies (SSTAs), associated with the El Niño/Southern Oscillation (ENSO), is transferred into midlatitudes to drive SSTAs remotely with the opposite sign [*Lau and Nath,* 1994, 1996, 2001; *Lau,* 1997; *Alexander et al.,* 2002, 2004; *Hoerling and Kumar,* 2002]. A similar mechanism must be operative also in decadal SST variability over the North Pacific driven by tropical variability [*Nitta and Yamada,* 1989; *Trenberth,* 1990]. Pacific decadal variability is reviewed by *Seager et al.* [2004]. Once a stationary atmospheric teleconnection pattern forms in response to tropical SSTAs with equivalent barotropic anomalies at midlatitudes, local storm track activity and associated poleward heat transport are altered [*Trenberth,* 1990; *Hoerling and Ting,* 1994]. It is this anomalous heat flux through which anomalous upper-level westerly momentum is transferred to the surface. Surface wind anomalies thus enhanced drive SSTAs locally by changing surface turbulent heat fluxes, entrainment at the oceanic mixed-layer bottom, and a cross-frontal Ekman current [*Frankignoul and Reynolds,* 1983; *Frankignoul,* 1985; *Alexander,* 1992; *Miller et al.,* 1994].

The ocean–atmosphere interaction in the "atmospheric bridge" paradigm is thus primarily one-way forcing by atmospheric anomalies on the upper ocean. Thus, local correlation must be *negative* between SST and upward turbulent flux anomalies [*Cayan,* 1992ab; *Hanawa et al.,* 1995; *Tanimoto et al.,* 1997; *Alexander et al.,* 2002], and so is the local correlation between a SSTA and anomalous surface wind speed. Midlatitude SSTAs thus generated tend to have large horizontal extent, reflecting the spatial scale of atmospheric anomalies that have forced them [*Namias and Cayan,* 1981; *Wallace and Jiang,* 1987]. The one-way nature is consistent with the fact that most of the atmospheric general circulation models (AGCMs) fail to generate systematic response to prescribed midlatitude SSTAs [*Kushnir et al.,* 2002]. Several experiments, however, in each of which an AGCM is coupled thermally with a slab ocean mixed layer model [*Lau and Nath,* 1996, 2001; *Watanabe and Kimoto,* 2000] showed that midlatitude SSTAs can reinforce atmospheric anomalies that have driven them. This weak local feedback is called "reduced thermal damping" [*Kushnir et al.,* 2002], as elucidated by *Barsugli and Battisti* [1998] in a linearized one-dimensional coupled model.

### *2.2. Oceanic influence from western-basin frontal zones*

As discussed above, the atmospheric forcing dominates in the coupled variability over the vast central and eastern domains of a basin. SSTA formation, however, cannot be interpreted solely with local exchanges of heat and momentum through the surface around western boundary currents, where the oceanic thermal advection is substantial in the upper-ocean heat budget [*Qiu and Kelly,* 1993; *Qiu,* 2000, 2002; *Kelly and Dong,* 2004]. Thus, the role of SSTAs in air–sea interaction can be more than the "reduced thermal damping". In fact, *Nonaka and Xie* [2003] found the SST–wind correlation in satellite data to be *positive* along the Kuroshio and its extension [*Xie,* 2004], indicative of modification in near-surface stratification by underlying SSTAs. Analyzing wintertime shipboard measurements compiled on a high-resolution grid over the North Pacific, *Tanimoto et al.* [2003] found that turbulent heat flux anomalies are *positively* correlated with SSTAs in the subarctic frontal zone located in the Kuroshio-Oyashio Extension [*Yasuda et al.,* 1996; *Yuan and Talley,* 1996], and that the positive correlation is stronger when the SSTAs lead the flux anomalies. Confined to a meridionally narrow region along the Kuroshio or frontal zone, the signal of this oceanic thermal forcing would hardly be captured in data complied on a coarse resolution grid (with ~5? latitudinal intervals) or through a statistical method that preferentially extracts basin-scale anomaly patterns such as a singular-value decomposition used by *Deser and Timlin* [1997] and others.

A close association has been found in the extratropics between frontal zones and decadal SST variability [*Nakamura et al.,* 1997a; *Nakamura and Yamagata,* 1999; *Nakamura and Kazmin,* 2003]. *Schneider et al.* [2002] argued that the Kuroshio Extension could be the key region for oceanic feedback on the atmosphere for the Pacific decadal variability, although the associated frontal zone is unlikely to be resolved in their model. *Tanimoto et al.* [2003] argued how SSTAs observed in the frontal zone with decadal variability inherent to the North Pacific [*Deser and Blackmon,* 1995; *Nakamura et al.,* 1997a; *Nakamura and Yamagata,* 1999; *Xie et al.,* 2000; *Tomita et al.,* 2001] can reinforce associated stationary atmospheric anomalies. Their results are summarized in Figure 1, Plates 1 and 2. In the presence of warm (cool) SSTAs in early part of winter (Plate 1a), latent heat release is enhanced (reduced) along the frontal zone (Figure 1; Plate 2a). Linearization of heat flux anomalies [*Halliwell and Mayer,* 1996] reveals that the enhanced (reduced) heat release is attributed to the effect of the local SSTAs (Figure 1; Plate 2b), part of which is offset by a contribution from surface air-temperature (and moisture) anomalies (Figure 1; Plate 2c). A contribution from wind anomalies is negligible in the subarctic

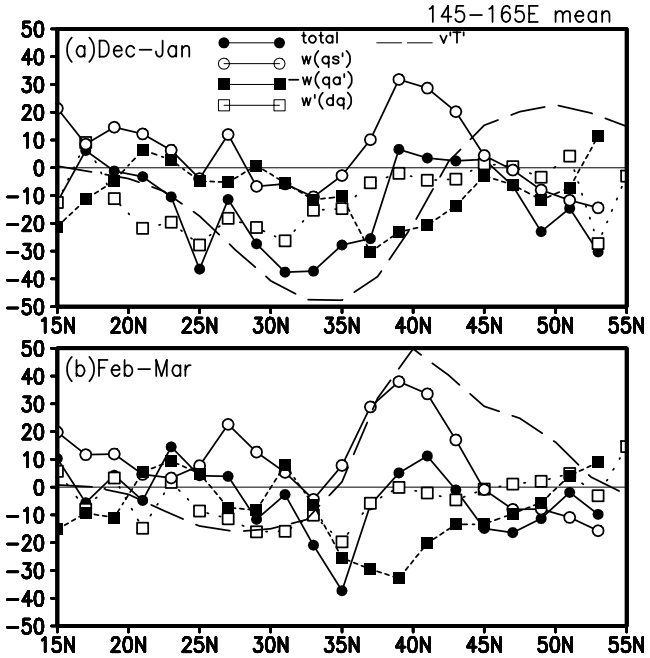


**Figure 1.** Meridional profiles of anomalous upward latent heat flux (W $m^{-2}$; solid line with closed circles; upward positive) at the surface, as an average between 145°E and 165°E, for (a) Dec.–Jan. and (b) Feb.–Mar. The subarctic frontal zone is between 36°N and 44°N. Superimposed are individual contributions to the total anomalous flux solely from (and proportional to) local SSTAs (solid line with open circles), anomalous air temperature (dotted line with closed squares) and anomalous surface wind speed (dotted line with open squares). Anomalous 850-hPa poleward heat flux associated with subweekly eddies (unit: 10 K m $s^{-1}$; long dashed line), as an average over the same longitudinal sector, is also superimposed. These profiles are based on the anomalies shown in Plate 2.

frontal zone (Figure 1; Plate 2d). As shown in Plate 2e, the local storm track is displaced poleward (equatorward), probably in response to changes in near-surface baroclinicity, as consistent with the observed decadal shift of the frontal axis [*Nakamura and Kazmin,* 2003]. This tendency is obvious particularly in early winter, as the eddy heat flux is enhanced (reduced) where the anomalous SST gradient is enhanced (relaxed) as in Figure 1a. In the upper troposphere, the anomalous storm track activity exerts anticyclonic (cyclonic) forcing over the midlatitude North Pacific through anomalous vorticity transport (Plate 2f), reinforcing the pre-existing stationary anticyclonic (cyclonic) anomalies. Consistent with this eddy forcing, a wave-activity flux of stationary Rossby waves [*Takaya and Nakamura,* 2001] is strongly divergent from the anomalies that resemble the Pacific/North American (PNA) pattern [*Wallace and Gutzler,* 1981], which is regarded as a preferred mode of variability in the exit of the North Pacific jet [*Simmons et al.,* 1983; *Peng and Robinson,* 2001]. As in the "atmospheric bridge", anomalous westerly momentum associated with the PNA pattern is transferred downward by eddies, to reinforce the anomalous surface Aleutian low (Plate 1e). Surface wind anomalies thus reinforced exert thermal forcing upon the upper ocean over the central and eastern North Pacific, acting to extend warm (cool) SSTAs downstream of the frontal zone and drive cool (warm) SSTAs off western Canada, in a manner consistent with the observed tendency in SSTAs to late winter (Plates 1a-c).

*Kushnir et al.* [2002] have postulated a similar mechanism as a paradigm for the coupling between a meridional dipole of atmospheric stationary anomalies and dipolar SSTAs as typically observed in the North Atlantic. Again, a critical factor in forcing the atmospheric anomalies is anomalous storm track activity in response to changes in surface baroclinicity associated with the SSTAs. They considered a particular situation where the SSTAs have been generated by the atmospheric anomalies, as in the "atmospheric bridge". In contrast, over the decadal SSTAs observed in the Pacific subarctic frontal zone, surface wind anomalies are weak, especially in early winter (Plate 1d), indicative of greater importance of oceanic processes [*Xie et al.,* 2000]. It has been suggested that SST variations around the Kuroshio Extension are strongly influenced by changes in oceanic condition [*Tomita et al.,* 2002; *Qiu,* 2003; *Kelly and Dong,* 2004], including the gyre adjustment to atmospheric forcing exerted far to the east [*Schneider et al.,* 2002]. Once zonally elongated SSTAs form in a frontal zone through oceanic processes, they would act to modify the surface baroclinicity locally.

Owing to the two-way interactive nature, a more convincing argument on the oceanic influence on atmospheric anomalies requires modeling studies. Part of the mechanisms argued by *Tanimoto et al.* [2003] is essentially the same as what *Peng and Whitaker* [1999] suggested from their careful diagnosis of an AGCM response to warm SSTAs in the Pacific subarctic frontal zone. They revealed the critical importance of a local storm track in yielding a PNA-like stationary atmospheric response in barotropic structure. A similar suggestion was made by *Watanabe and Kimoto* [2000] for the North Atlantic variability. *Peng and Whitaker* [1999] showed that their AGCM response is sensitive to subtle differences in the model time-mean flow. The sensitivity stems from how effectively the baro-tropic response is excited under the storm track feedback from near-surface anomalies as the robust direct response to the SSTAs. Since the SSTA pattern given in the model was taken from the observation, a mismatch could happen in their positions between the model storm track and the direct thermal response. The model sensitivity suggests the potential importance of their association, though may not be quite robust, between the frontal zone and storm track in reinforcing the PNA-like anomalies. The association may be part of

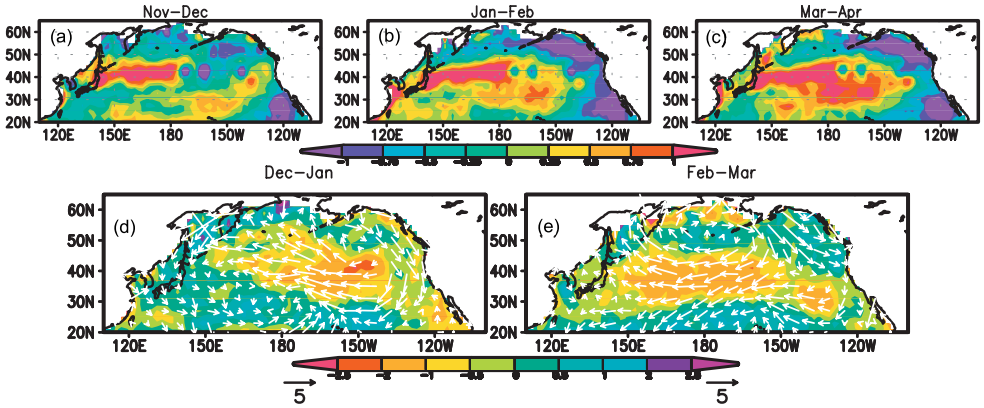


**Plate 1.** Difference maps of bi-monthly SSTA (°C; reddish and bluish colors for warm and cool anomalies, respectively, as shown below the panels) associated with the North Pacific decadal variability between 4-year composites for 1968/69~1971/72 and 1982/83~1985/86 (i.e., "warm" minus "cold"). Based on the Comprehensive Ocean–Atmosphere Data Set (COADS) complied on a 2°?2° lat.–lon. grid for (a) Nov.–Dec., (b) Jan.–Feb. and (c) Mar.–Apr. (d) As in (a), but for surface wind velocity (arrows with scaling below the panels) and scalar wind speed (m $s^{-1}$; bluish and reddish colors for stronger and weaker winds, respectively, as shown below the panels) for Dec.–Jan. (e) As in (d), but for Feb.–Mar. After *Tanimoto et al.* [2003].

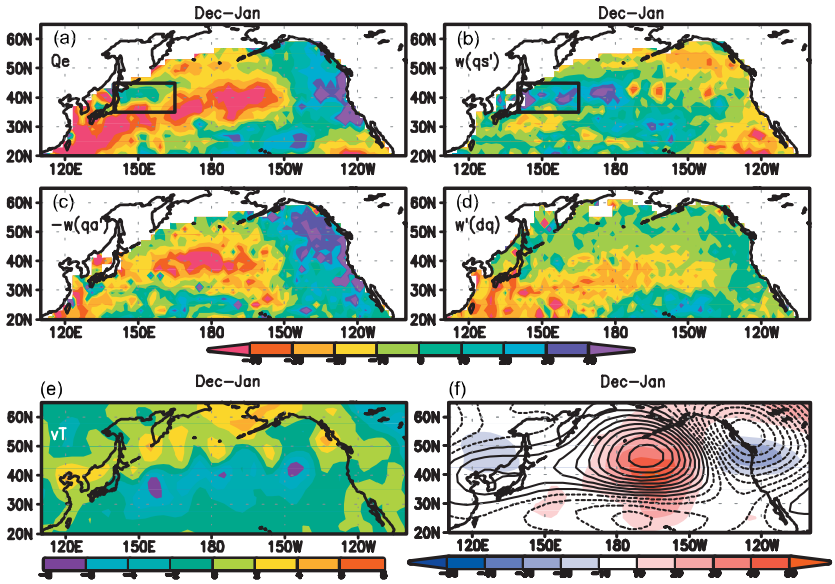


**Plate 2.** (a) As in Plate 1, but for Dec.–Jan. total upward latent heat flux anomalies at the surface (W $m^{-2}$; bluish and reddish colors for enhanced and reduced heat release, respectively, from the ocean). The subarctic frontal zone is indicated with a rectangle. (b) As in (a), but for a contribution only from local SSTAs, based on linearization applied to the total anomalous flux in (a). (c) As in (b), but for a contribution only from local air temperature anomalies. (d) As in (b), but for a contribution only from local wind speed anomalies. (e) As in (a), but for storm track activity measured by 850-hPa poleward heat flux associated with subweekly eddies (K m $s^{-1}$; reddish and bluish colors for the flux enhancement and reduction, respectively), based on the NCEP/NCAR reanalyses. (f) As in (e), but for 250-hPa height (contoured with 20-m intervals), superimposed on feedback forcing from anomalous storm track activity measured by 250-hPa geopotential height tendency (m $day^{-1}$; bluish and reddish colors for the cyclonic and anticyclonic tendencies, respectively) due only to eddy vorticity flux convergence [*Nakamura et al.,* 1997b]. After *Tanimoto et al.* [2003]. Coloring conventions are shown below the panels.

a feedback loop that is likely operative in the decadal variability inherent to the North Pacific.

## 3. CLIMATOLOGICAL ASSOCIATIONS AMONG STORM TRACKS, POLAR-FRONT JETS AND MIDLATITUDE OCEANIC FRONTS

### *3.1. Southern Hemisphere (SH)*

Figure 2 shows the SH climatology of storm track activity, westerly wind speed and SST gradient. A prototype example of a close association among a subarctic frontal zone, midlatitude storm track and polar-front jet can be found around 50?S especially in austral summer [Figures 2d-f; *NS04*]. In winter, the association is still close over the South Atlantic and Indian Ocean (Figures 2a-c). There the low-level storm track activity is stronger than over the South Pacific, which seems in correspondence with tighter SST gradient across the Antarctic Polar Frontal Zone (APFZ) [*Colling,* 2001], a subarctic frontal zone along the Antarctic Circumpolar Current (ACC), over the former oceans. Along that frontal zone, a strong baroclinic zone forms near the surface (Fig-

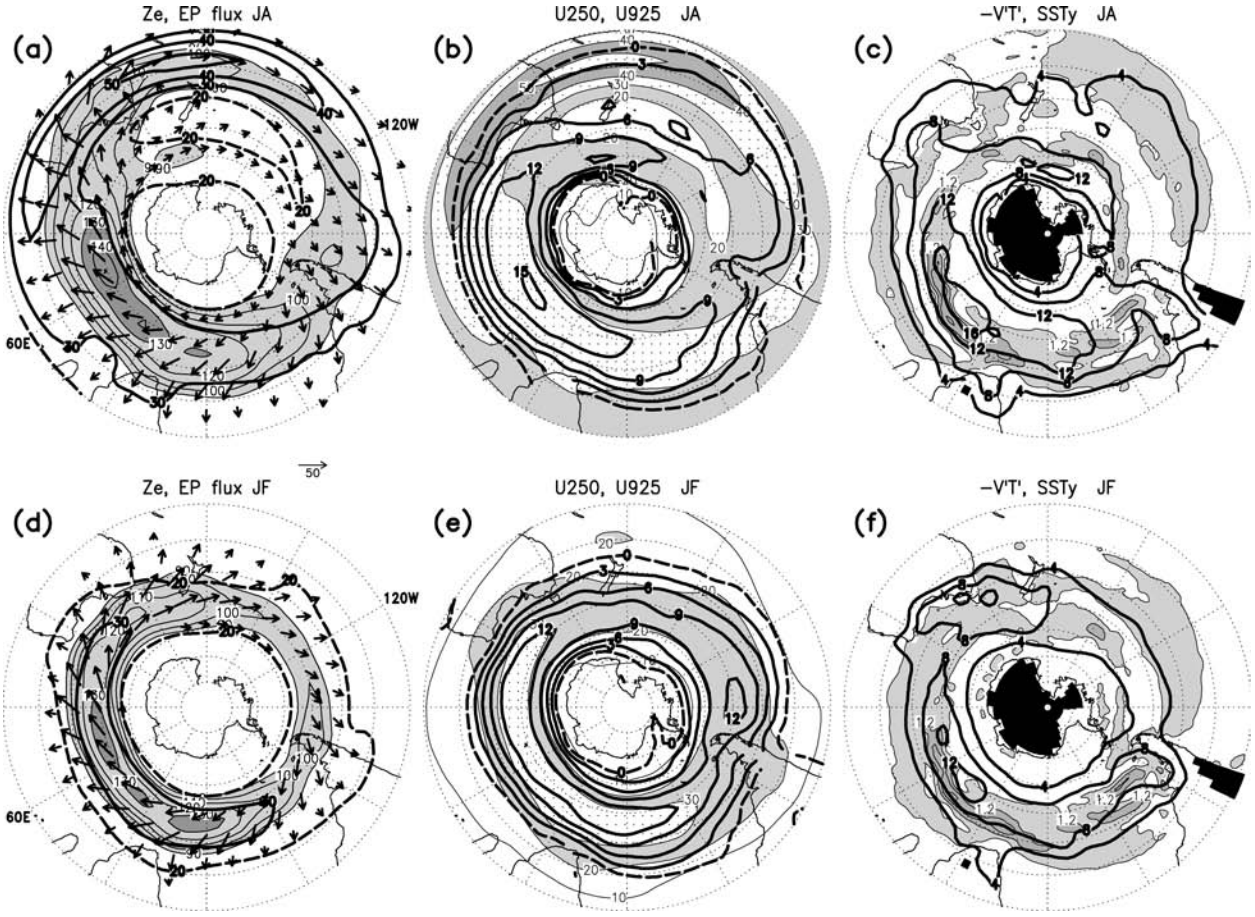


**Figure 2.** (a) Climatological Jul.–Aug. distribution for the upper-level SH storm track activity (stippling) and horizontal component of 250-hPa extended E-P flux (arrows indicating eddy transport of mean-flow easterly momentum; scaling at the bottom: unit: $m^2\ s^{-2}$), with 250-hPa westerly wind speed ($U$ : $m\ s^{-1}$; heavy solid lines for 30, 40, 50 and 60; heavy dashed line for 20). Light and heavy stippling is applied where amplitude of subweekly fluctuations in geopotential height ($Z_e$: m) at the 250-hPa level is between 90 and 130 and above 130, respectively, with thin lines for every 10. Based on the NCEP (National Centers for Environmental Prediction) reanalyses. (b) As in (a) but for 925-hPa $U$ ($m\ s^{-1}$; heavy lines for 3, 6, 9, 12 and 15; dashed for $U = 0$) and 250-hPa $U$ ($m\ s^{-1}$; light stippling for 20~30; heavy stippling for 40~50). (c): As in (a), but for 850-hPa poleward heat flux associated with subweekly eddies (heavy lines for 4, 8, 12 and 16 K $m\ s^{-1}$). Light and heavy stippling indicates oceanic frontal zones where meridional SST gradient (°C/110 km) exceeds 0.6 and 1.2, respectively (thin lines are drawn for every 0.6), based on satellite and shipboard data complied by *Reynolds and Smith* [1994]. Dark shading indicates data-void regions. (d–f) As in (a–c), respectively, but for Jan.–Feb.

ures 3d-e). Both in the upper and lower troposphere (Figure 2), the storm track core forms in the southwestern Indian Ocean, almost coinciding with the core of the APFZ. In fact, *Sinclair* [1995] found that the most frequent cyclogenesis in the SH occurs around this APFZ core. There, in the course of the seasonal march, the low-level storm track activity exhibits high positive correlation with baroclinicity for a layer just above the surface. *NS04* showed that the correlation is even higher than that with the baroclinicity near the steering (700~850 hPa) level of subweekly eddies, which is also the case for the South Atlantic. Meridional sections in Figures 3d-e show a deep structure of the storm track over the Atlantic and Indian Ocean. The structure reflects the pronounced baroclinic eddy growth above the intense surface baroclinic zone and the downstream development of eddies along the upper-level polar-front jet that acts as a good waveguide for baroclinic wavepackets (Figures 3a-b). In fact, the extended Eliassen-Palm (E-P) flux [*Trenberth,* 1986] has a strong eastward component in the core of the upper-level storm track [*NS04*]. The jet is the sole westerly jet in summer. Even in winter when a subtropical jet intensifies, the storm track core over the South Indian Ocean remains preferentially along the polar-front jet (Figure 2).

The SH storm track core is collocated with the core of the surface westerly jet (Figure 2) as part of the deep polar-front jet (Figures 3a-b) maintained mainly by the downward transport of mean-flow westerly momentum via eddy heat fluxes. The fact that the strongest annual-mean wind stress within the world ocean is observed around the SH storm core [*Trenberth et al.*, 1990] suggests the importance of the storm track activity in driving the ACC and associated APFZ. As shown in Figures 4b and 4d, the annually averaged surface westerly acceleration induced as the feedback forcing through heat and vorticity transport by subweekly eddies is indeed strong along or slightly poleward of the surface westerly axis, and it is strongest near the core of the APFZ. The slight poleward displacement of that axis relative to the APFZ (Figure 2) seems consistent with a tendency for surface upward turbulent heat

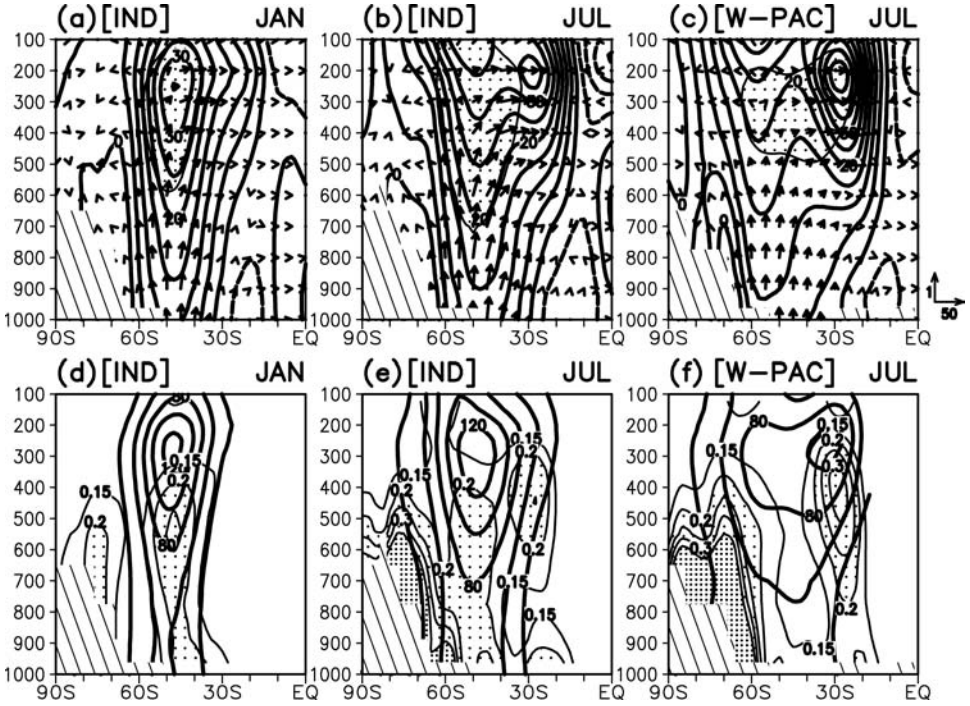


**Figure 3.** (a) Climatological Jan. section of meridional ($m^2\ s^{-2}$) and vertical (Pa m $s^{-2}$; proportional to poleward eddy heat flux) components of the extended E-P flux (arrows; scaling at the lower-right corner), and $U$ (contour ed for every 5 m $s^{-1}$; dashed for the easterlies), both for the South Indian Ocean (50°~90°E). Based on the NCEP reanalyses. (b) As in (a) but for July. (c) As in (a) but for Jul. in the Australian sector (120°~ 160°E). Hatching indicates topography. (d–f) As in (a–c), respectively, but for eddy amplitude in geopotential height ($Z_e$; unit: m; heavy lines for every 20 from 40) and local baroclinicity ($G$; thin lines for every 0.05 from 0.15; light stippling for 0.2~0.35 and heavy stippling for above 0.35). Here, $G = |g/f_0|\bullet|\nabla\theta/(\theta N)$*, where N denotes the Brunt-Väisälä frequency,* $\theta$ potential temperature, $g$ the acceleration of gravity, $f$ the Coriolis parameter and $f_0 = f$ (45°S). In linear theories of baroclinic instability for the zonally uniform westerlies, the maximum growth rate of the most unstable mode is proportional to $G$. In (a–c), stippling for $Z_e > 80$ (m). After *NS04*.

fluxes, wind stirring effect on the oceanic mixed layer, and Ekman velocity to be all maximized along the wind velocity axis. Consistent with an evaluation by *Lau and Holopainen* [1984] for the NH, a contribution from eddy heat transport is stronger than that from eddy vorticity transport, but their contributions are more comparable (not shown).

Over the South Pacific, the association among a midlatitude storm track, polar-front jet and subarctic frontal zone is less robust than over the Atlantic and Indian Ocean [*NS04*]. Though vulnerable to the seasonal intensification of a subtropical jet, their close association can still be found in austral summer and autumn when the jet is diminished. In these seasons, the Pacific storm track at the upper and lower levels is part of a well-defined circumpolar storm track along the ~50?S circle, accompanied consistently by the deep polar-front jet (Figures 2d-f). The low-level eddy activity gradually weakens downstream across the Pacific, as the SST gradient relaxes eastward along the APFZ (Figure 2f). The close association was observed also in a very unusual winter at the beginning of the 1998 La Niña event, in the absence of the intense subtropical jet due to the marked interannual variability. In that winter, the upper-level westerly bifurcation was much less apparent than in the climatology, which marks a sharp contrast with a distinct double-jet structure in the previous winter, as in other El Niño winters [*Chen et al.,* 1996]. As well inferred from a difference map in Figure 5a, no well-defined storm track formed over the subtropical South Pacific in the 1998 winter, under the extremely weakened subtropical jet. Instead, eddy activity over the South Pacific was enhanced at midlatitudes and organized into a single storm track along the polar-front jet at ~55?S throughout the troposphere (Figure 5), which indeed resembled the summertime situation (Figure 2). In 1998, the midlatitude westerlies were stronger not only in the upper troposphere but also near the surface (Figure 5), consistent with coherent vertical structure of the midlatitude storm track. In that winter, upper-level wave activity was dispersed strongly equatorward from the enhanced subpolar storm track in the central and eastern Pacific, through which the westerly momentum was transported poleward. Its downward transfer by eddies sustained the strong surface westerlies. In a macroscopic view, the Pacific APFZ remained similar between the two winters, seemingly to keep anchoring the low-level storm track and polar-front jet (not shown).

### *3.2. Northern Hemisphere (NH)*

Figure 6 shows the NH climatology of storm track activity, westerly wind speed and SST gradient. Over each of the ocean basins, a major storm track extends eastward from an intense surface baroclinic zone anchored along a subarctic frontal zone off the western boundary of the basin (Figure 6b), where warm and cool boundary currents are confluent. In a macroscopic view, the storm track is along the boundary between subtropical and subpolar gyres. In addition, the thermal contrast between a warm boundary current (the Gulf Stream or Kuroshio) and its adjacent cooler landmass also influences the storm track activity in winter [*Dickson and Namias,* 1976; *Gulev et al.,* 2003]. Over the North Atlantic, a belt of the surface westerlies between the Icelandic Low and Azores High is situated slightly to the south of the storm track axis. Over the wintertime North Pacific, the poleward displacement of the low-level storm track relative to the surface westerly axis is more apparent. The latter is closer to the subtropical jet axis aloft especially over the western Pacific, although the poleward secondary branch of the surface westerlies is close to the storm track.

Despite the modest intensity of the local upper-level westerly jet (Figure 6a), midwinter storm track activity is stronger

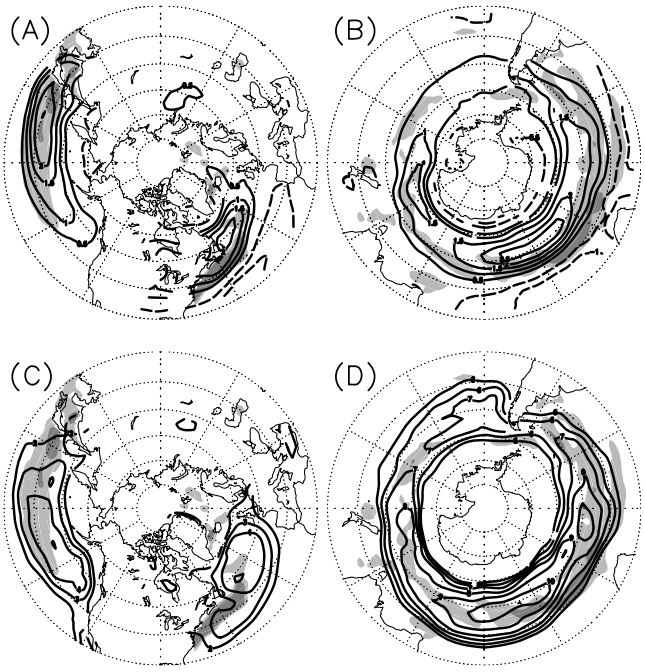


**Figure 4.** (a) Climatological annual-mean westerly acceleration (solid lines at 0.5 m $s^{-1}$ $day^{-1}$ intervals with zero lines omitted; dashed lines for easterly acceleration) at the 1000-hPa level over the NH, as the feedback forcing from storm tracks evaluated in the same manner as in *Lau and Holopainen* [1984] but based on 8-day high-pass-filtered NCEP reanalysis data for 1979~98. Light and heavy stippling indicates oceanic frontal zones where climatological annual-mean meridional SST gradient (°C/110 km) is 0.8~1.6 and above 1.6, respectively, based on the data by *Reynolds and Smith* [1994]. (b) As in (a) but for the SH. (c) As in (a) but for the 1000-hPa westerly wind speed for the NH (solid lines for 2, 3, 4 and 5 m $s^{-1}$). (d) As in (a) but for the 1000-hPa westerly wind speed for the SH (solid lines for 5, 6, 7 8, 9 and 10 m $s^{-1}$).

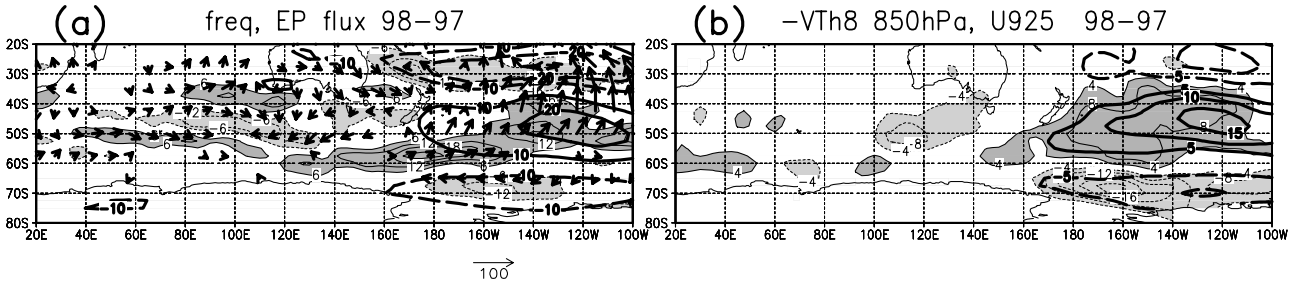


**Figure 5.** Difference maps over the South Indian and Pacific Oceans for Jul.~Aug. between 1997 and 1998 (1998 minus 1997). (a) Horizontal component of 250-hPa extended E-P flux (arrows; scaling at the bottom; unit: $m^2\ s^{-2}$) associated with subweekly eddies, 250-hPa *U* (heavy lines for 10, 20 and 30 m $s^{-1}$; dashed for the anomalous easterlies) and 250-hPa storm tracks (stippling). Light and heavy stippling is applied where decrease and increase, respectively, in the frequency of an eddy amplitude maximum passing through a given data point with 2.5° intervals on a given meridian, defined as the number of days over a 62-day period, exceed 6 (thin lines for every 6). (b) 925-hPa *U* (heavy lines for 5, 10 and 15 m $s^{-1}$; dashed for the anomalous easterlies) and 850-hPa poleward eddy heat flux (K m $s^{-1}$; light contours for every 4; light and heavy stippling for positive and negative values). Based on the NCEP reanalyses.

over the North Atlantic than over the North Pacific (Figure 6b). The low-level storm track axis is closer to a subarctic frontal zone in the Atlantic than in the Pacific, and the cross-frontal SST gradient is substantially stronger in the Atlantic than in the Pacific (Figure 6b). While its main surface axis extends along the Oyashio Extension at ~42?N, the North Pacific subarctic frontal zone at the surface is meridionally broader, including the Interfrontal Zone in the Kuroshio-Oyashio Extension [*Lin and Talley,* 1996; *Yasuda et al.,* 1996; *Nakamura and Kazmin,* 2003]. The North Atlantic subarctic frontal zone is shaper and more intense, contributing to the more pronounced local eddy growth and perhaps to the stronger eddy activity.

Another factor that contributes to the Atlantic-Pacific difference in wintertime storm track activity is latitudinal displacement between a storm track and subarctic frontal zone. In the course of its seasonal march, the North Atlantic storm track stays to the north of the subarctic frontal zone, and it is nearest to the front in midwinter when eddy activity peaks (not shown). The westerly jet axis closely follows the underlying frontal zone, especially downstream of the jet core (Figure 6). The North Pacific storm track undergoes larger seasonal migration in its latitudinal position [*N92*], and eddy activity tends to be suppressed in midwinter when the storm track axis stays to the south of the Pacific subarctic frontal zone [*Nakamura and Sampe*, 2002; hereafter *NS02*]. *NS02* found that upper-level eddies traveling from the Asian continent tend to propagate above the surface baroclinic zone along the frontal zone when the storm track activity peaks in spring and late fall [*N92*]. In those seasons, the upper-level westerly jet core is substantially weaker than in midwinter and located somewhat poleward [*NS02*]. The suppression occurs despite the fact that the tropospheric baroclinicity peaks in midwinter. *NS02* pointed out that midwinter eddy activity has enhanced substantially since the late 1980s, as the Pacific storm track tends to stay over the subarctic frontal zone under the decadal weakening of the subtropical jet. They found that, for most of the time during the recent midwinter periods, the eddy amplitude maximum stayed at the midlatitude tropopause right above the frontal zone (Figure 7a), which allowed eddies efficient baroclinic growth through their interaction with a surface baroclinic zone along the frontal zone, as in fall and spring. In fact, eddies exhibited a deeper structure with vigorous poleward heat transport (Figure 7a). In each of these situations over either the Atlantic or Pacific, the extended E-P flux is strongly divergent in the upper troposphere out of the storm track core (not shown). Thus, a westerly jet with modest core velocity bears an eddy-driven nature, a characteristic of a polar-front jet [*Lee and Kim*, 2003]. These results suggest that the association with the underlying frontal zones contributes to the enhancement of the NH storm track activity.

Despite pronounced seasonal march in the axial position and intensity of the NH storm tracks, especially over the Pacific, the annually averaged surface westerly acceleration induced as the feedback forcing from the storm tracks is strongest along the poleward flank of a subarctic frontal zone over each of the ocean basins (Figure 4a), driving oceanic gyres. In the winters of enhanced eddy activity (Figure 8a), the surface westerly axis was situated along the northern fringe of the subarctic frontal zone in the western Pacific, and it was systematically below the upper-level storm track axis over the eastern Pacific. *N92* showed that, in the course of the seasonal march, the axis of the low-level westerlies tends to follow the upper-level storm track over the eastern Pacific, indicative of the reinforcement of the westerlies by the storm track.

## 4. INFLUENCE OF A SUBTROPICAL JET ON A STORM TRACK AND ITS ASSOCIATION WITH AN OCEANIC FRONT

### *4.1. Southern Hemisphere (SH)*

In the SH climatology (Figure 2), the influence of the seasonal evolution of a subtropical jet stream on storm track activity is apparent only over the South Pacific [*NS04*]. Its wintertime intensification disturbs the association among a midlatitude storm track, polar-front jet and subarctic frontal zone observed over the South Pacific in austral summer and autumn. In the presence of double-jet structure [*Karoly et al.,* 1998; *Bals-Elsholz et al.,* 2001], upper-tropospheric storm track activity bifurcates from the core region into the main branch along the strong subtropical jet and the sub-branch along the weaker polar-front jet (Figure 2a). Thus, the westerlies and storm track are no longer circumpolar. The intense velocity core of the subtropical jet confined to the tropopause (Figure 2c) acts as an excellent waveguide for synoptic-scale eddies. In fact, the extended E-P flux associated with subweekly eddies is consistently eastward along the jet (Figures 2a). Located above a surface subtropical high-pressure belt, however, the jet does not favor baroclinic eddy growth, despite the modest surface baroclinicity across the underlying subtropical frontal zone (Figure 2c). Consistently, the subtropical jet does not accompany the strong westerlies at the surface (Figure 2b), thus yielding no significant contribution to the local mechanical driving of the ocean circulation. Over the extratropical SH, the annual-mean surface westerly acceleration induced as eddy feedback forcing is weakest over the South Pacific (Figure 4b), due to the winter-spring breakdown of the well-defined midlatitude storm track.

In winter and spring, the main branch of the low-level storm track is still along the polar-front jet (Figures 2b-c), though displaced poleward above an enhanced low-level baroclinic zone that forms along the seasonal sea-ice margin (Figure 3f). The low-level storm track forms despite the upper-level wave activity from upstream core region is mostly dispersed toward the subtropical jet (Figures 2a and 3b), suggestive of the importance of surface baroclinicity in the storm track formation.

### *4.2. Northern Hemisphere (NH)*

A factor that contributes to the Atlantic-Pacific difference in storm track activity is the midwinter eddy-activity minimum (suppression) in the North Pacific [*N92*]. As opposed to linear theories of baroclinic instability [*Charney*, 1947; *Eady*, 1949], this unique aspect of the seasonal cycle occurs despite the local westerly jet is strongest in midwinter. *Bosart* [1999] speculated critically that the minimum might merely be an artifact due to the sampling by *N92* on the 250-hPa surface that tends to be above the tropopause only in midwinter. However, his speculation is inconsistent with the activity minimum also observed at the lower levels [*N92*; *Nakamura et al.,* 2002]. The minimum has been reproduced in AGCMs [*Christoph et al.,* 1997; *Zhang and Held,* 1999; *Chang,* 2001]. In reanalysis data, *Nakamura et al.* [2002] found the activity

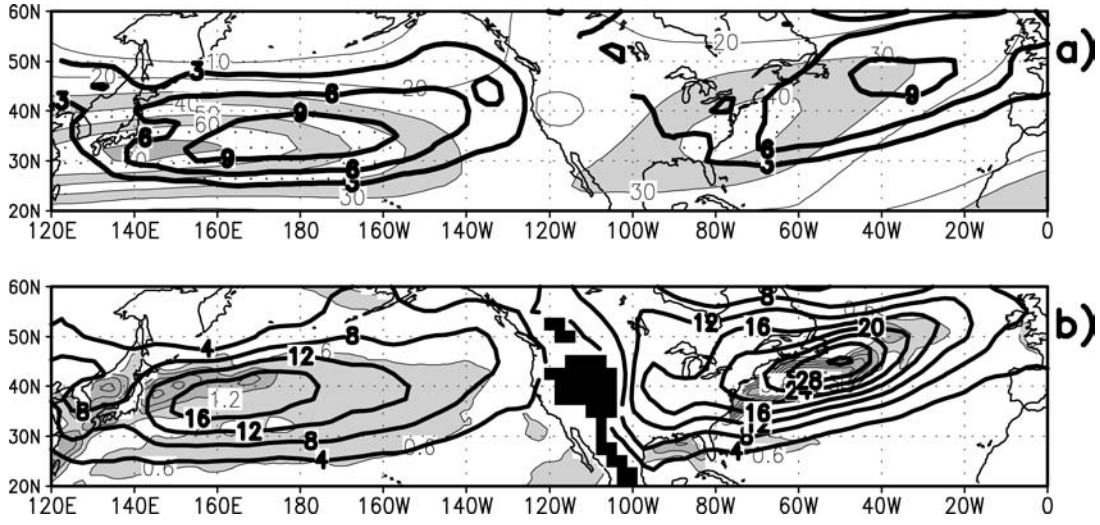


**Figure 6.** (a) Climatological Jan.~Feb. distribution of 925-hPa *U* (heavy lines for every 3 m $s^{-1}$) and 250-hPa *U* (light and heavy stippling for 30~40 and 50~60 m $s^{-1}$, respectively), based on the NCEP reanalyses. (b) As in (a) but for 850-hPa poleward eddy heat flux (heavy lines for every 4 K m $s^{-1}$). Light and heavy stippling indicates oceanic frontal zones where meridional SST gradient (°C/110 km) is 0.6~1.2 and above 1.2, respectively (with thin lines for every 0.6), based on the data by *Reynolds and Smith* [1994].

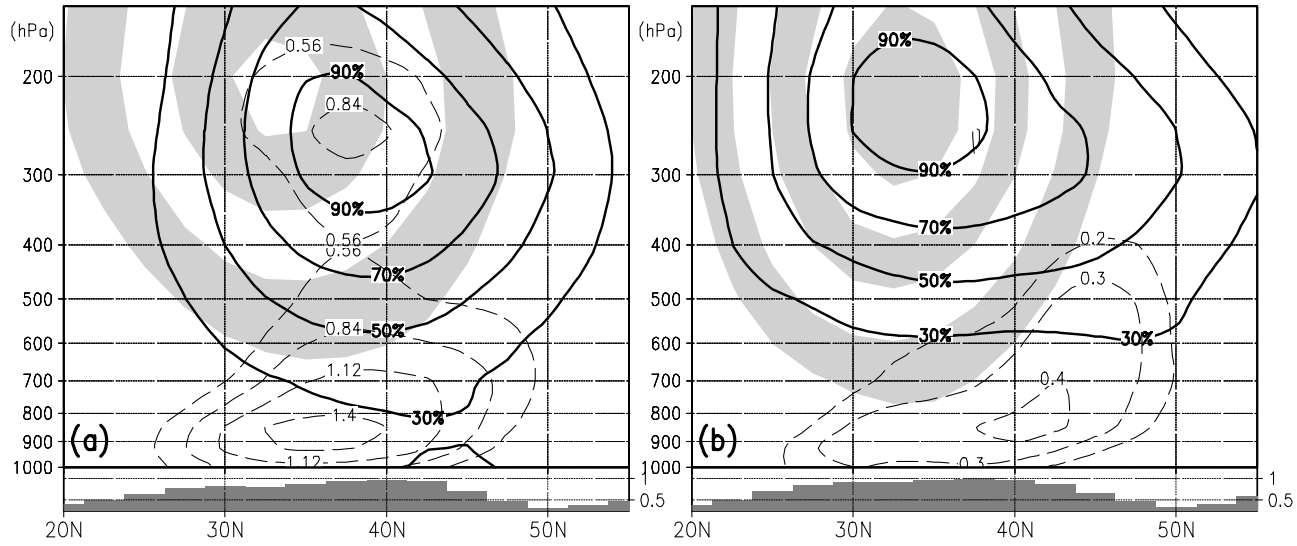


**Figure 7.** Meridional structure of a typical baroclinic eddy in the North Pacific storm track (170°E~170°W). Based on subweekly fluctuations in geopotential height (*Z'*) field regressed linearly on 300-hPa *Z'* at [47°N, 105°E] with a 2-day lag, for (a) five Jan.~Feb. periods in 1979~95 with the weakest suppression in eddy activity and for (b) other five periods with the most distinct suppression. Reflecting the decadal weakening in the winter monsoon, the winters for (a) were all since 1987, whereas those for (b) were mostly before 1987. Eddy amplitude in *Z'* is normalized by its maximum (30, 50 70 and 90%). Associated poleward heat flux based on the regression (K m $s^{-1}$; density adjusted) is plotted with dashed lines for 0.56, 0.84, 1.12 and 1.40 in (a) and 0.2, 0.3 and 0.4 in (b). Note that eddy amplitude is larger in (a) by 67%. The westerly jet is indicated with stippling (*U*: 20~30, 40~50 and 60~70 m $s^{-1}$), and meridional SST gradient is plotted at the bottom (°C/110 km). Based on the NCEP reanalyses. After *NS02*.

minimum, which had been found by *N92* for 1965~84, has disappeared since the late 1980s, under the decadal weakening of the East Asian winter monsoon and associated relaxing of the subtropical jet. This modulation has been confirmed in *Chang's* [2003] analysis of unassimilated aircraft and rawinsonde data. As the mechanism of the activity suppression, *Chang* [2001] argued that enhanced precipitation in out-breaking cold air behind individual cyclones in mid-winter does not favor the generation of eddy available potential energy. Alternatively, we argue in the following that the suppression can be interpreted as the dynamical influence of a seasonally intensified subtropical jet.

In the wintertime Far East, the low-level monsoonal northerlies and the enhanced subtropical jet aloft, as observed before the late 1980s, are associated with the marked deepening of a planetary-wave trough, and a polar-front jet tends to merge itself into the subtropical jet [*Mohri,* 1953]. By the northerly component behind the trough, upper-level eddies are driven strongly toward the intensified subtropical jet and then trapped into its core at ~32?N at the 200-hPa level. The core is ~12 km in altitude, ~3 km higher than the midlatitude tropopause (300 hPa) at which eddies have been propagating through the polar-front jet over the Asian continent. In fact, the storm track underwent greater equatorward excursion from its annual-mean position in five midwinter periods with the most distinct eddy-activity minimum than in five other midwinter periods without the minimum [*NS02*]. Trapped by the subtropical jet core, eddies were lifted up by ~3 km and then staying 500~800 km away from the surface baroclinic zone above the subarctic frontal zone at ~40?N (Figure 7b). Thus, eddy interaction with the surface baroclinic zone tended to be impaired, while eddies underwent substantial distortion in their structure. The coherency is thus lowered between subweekly fluctuations in temperature and the meridional or vertical wind component [*N92*; *Chang*, 2001; *Nakamura et al.,* 2002], leading to the less efficient energy conversion for eddy growth. As shown in a meridional section in Figure 7b, under the trapping, eddy amplitude rapidly decays downward and the associated heat flux was reduced by as much as 40%.

As in the South Pacific case discussed earlier, the North Pacific subarctic frontal zone remained very similar between the two types of winter regardless of the substantial changes in storm track activity (Figure 8). Only the noticeable difference is the slightly enhanced cross-frontal SST gradient for the winters with eddy-activity minimum, indicating that the anomalous surface baroclinicity was unlikely the reason for the observed changes in the activity. The axes of the upper- and lower-level storm tracks and surface westerlies were more

closely located along the subarctic frontal zones in the winters of stronger eddy activity (Figure 8a). Rather, the axis of the surface westerlies nearly followed the subtropical jet axis in the winters of the suppressed storm track activity (Figure 8b).

## 5. DISCUSSION

The association among a storm track, polar-front jet and a subarctic frontal zone (including the APFZ) seems crucial for two-way interaction between the midlatitude atmosphere and ocean, as exemplified in an observational study by *Tanimoto et al*. [2003] and in an AGCM experiment by *Peng and Whitaker* [1999] both on the decadal variability inherent to the North Pacific [*Nakamura et al.,* 1997]. Furthermore, the whole dynamical picture of storm tracks and polar-front jets, including the localization of their core regions, can unlikely be obtained without considering their interaction with the underlying ocean, as first argued by *HV90* and recently by *NS02, Inatsu et al.* [2003] and *NS04.* In particular, key aspects of seasonal variations of a storm track can be interpreted reasonably well from a viewpoint of how strongly its association with the underlying subarctic frontal zone is disturbed by the seasonal intensification of a subtropical jet [*NS02, NS04*]. From this viewpoint, an insight can be gained into the mechanisms that cause the "midwinter activity minimum" of the North Pacific storm track [*NS02*], a puzzling feature of its seasonal cycle that cannot be explained by linear theories of baroclinic instability. The recent disappearance of the activity minimum may be interpreted as the consequence of the decadal weakening of the subtropical jet. In the absence of such a marked change in the subtropical jet, even subtle changes in the Pacific storm track activity could be observed in response to decadal SST changes in the subarctic frontal zone from the late 1960s into the 1980s [*Tanimoto et al.,* 2003]. Of course, the total baroclinicity within the troposphere must be considered in interpreting the profound seasonal march in eddy amplitude along the NH storm tracks, as discussed by *HV90.* They also emphasized the latent heat release along the storm tracks also acts to anchor them by forcing the planetary wave pattern.

It is well known that differential radiative heating acts to restore the mean baroclinicity at midlatitudes against the relaxing effect by eddy heat transport, but it provides no clear explanation why such intense surface baroclinic zones as observed are maintained. A tendency for major maritime surface baroclinic zones to be placed near midlatitude oceanic frontal zones [*NS02, NS04*] suggests the effective restoring of the atmospheric baroclinicity, owing to the large thermal

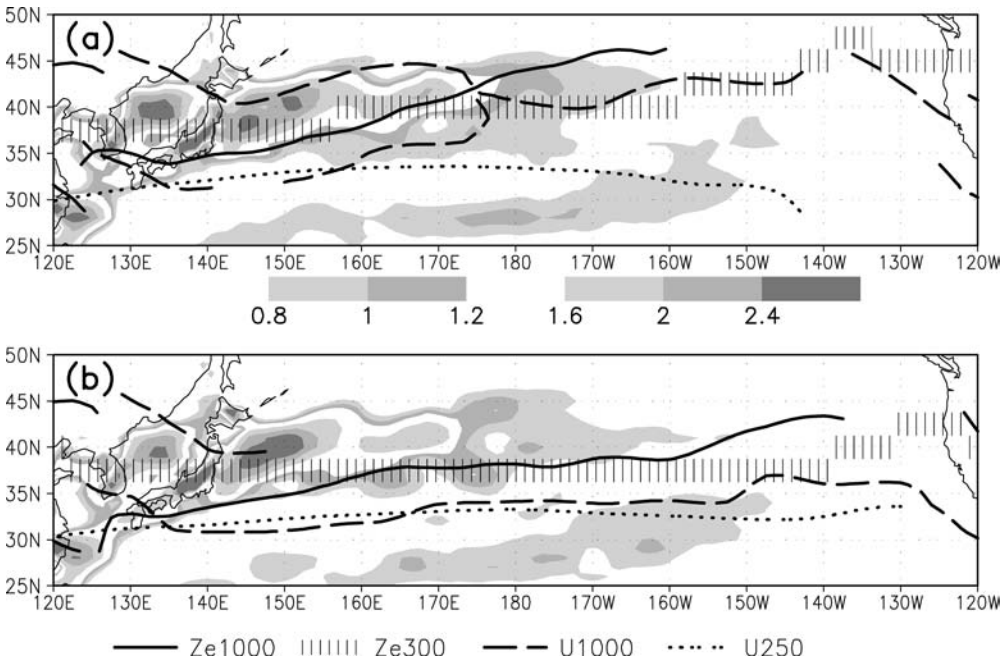


**Figure 6.** (a) Climatological Jan.~Feb. distribution of 925-hPa *U* (heavy lines for every 3 m $s^{-1}$) and 250-hPa *U* (light and heavy stippling for 30~40 and 50~60 m $s^{-1}$, respectively), based on the NCEP reanalyses. (b) As in (a) but for 850-hPa poleward eddy heat flux (heavy lines for every 4 K m $s^{-1}$). Light and heavy stippling indicates oceanic frontal zones where meridional SST gradient (°C/110 km) is 0.6~1.2 and above 1.2, respectively (with thin lines for every 0.6), based on the data by *Reynolds and Smith* [1994].

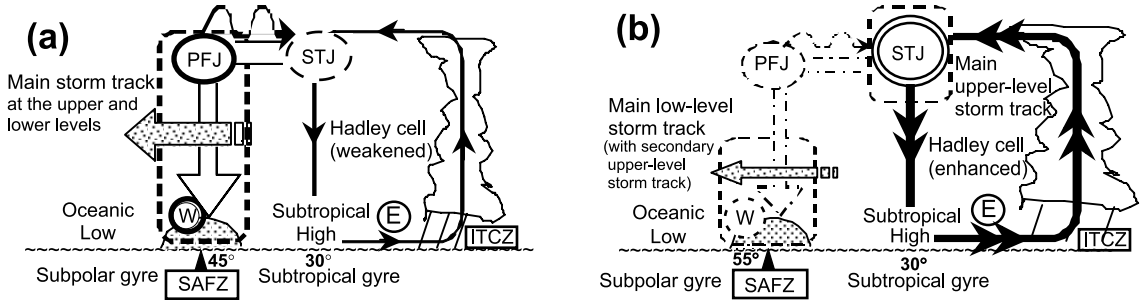


**Figure 9.** Schematics of different types of tropospheric general circulation over an ocean basin. (a) When a subtropical jet (STJ) is weak, the main storm track (thick dashed line) forms over a surface baroclinic zone (stippled at ~45° lat.) anchored by a subarctic frontal zone (SAFZ), as in the summertime SH, the North Atlantic or the North Pacific (in spring and fall). Wave-activity dispersion to the STJ (wavy arrow) leads to the formation of a deep polar-front jet (PFJ) above the SAFZ. Eddy downward transport (open arrow) of the mean-flow westerly momentum maintains a surface westerly jet (circled W) along the SAFZ. (b) When a STJ intensifies as in the wintertime South Pacific, the jet traps most of the upper-level eddy activity. Thus, the main branch of the upper-level storm track forms along the STJ with suppressed baroclinic eddy growth below, while the low-level storm track forms along a weak PFJ above a baroclinic zone anchored by the SAFZ.

inertia of the ocean mixed layer and the differential thermal advection between to the north and south of the frontal zones by strong oceanic currents [*Kelly and Dong*, 2004]. Enhanced heat and moisture fluxes over a warm current just south of a subarctic frontal zone has been known to contribute to cyclogenesis and thus storm track formation [*HV90*]. In addition, a sharp decline of the surface heat release poleward across the frontal zone acts to restore the mean atmospheric near-surface baroclinicity, thus also contributing to the anchoring of the storm track. This anchoring, however, can be disturbed by the seasonal intensification of a subtropical jet or its interannual modulations due to a teleconnection from the tropics or an upstream continent. An important scientific issue to be clarified is how the near-surface baroclinicity is determined and maintained in the marine boundary layer.

Another important aspect of the air–sea coupling associated with a storm track is that the mean westerly momentum carried downward with upward wave-activity transfer in a storm track is organized into a surface westerly jet, which drives oceanic gyres (or the ACC) and thereby contributes to the maintenance of subarctic frontal zones. Along the ACC, the core regions of the storm track, surface westerlies and APFZ almost coincide with each other, indicative of the presence of a local feedback loop. Over each of the NH ocean basins, the frontal zone is located at the confluent region of the western boundary currents driven mainly through gyre adjustment by the surface westerlies that are strongest farther to the east (Figure 4c). A storm track acts to maintain the westerlies, especially along or slightly to the north of the subarctic frontal zones (Figure 4a). The surface westerlies along the storm track also enhance the surface evaporation, whereas precipitation associated with migratory storms largely determines the fresh water supply to the midlatitude ocean [*Lukas,* 2001]. Kinetic energy input into the ocean by the strong surface westerlies and vigorous storm activity acts to sustain the mixed layer structure. The input also becomes an important source of oceanic turbulence available for deep-layer mixing [*Nagasawa et al.,* 2000].

Findings in this and related papers [*NS02, NS04*] may require some modifications to conceptual models for the zonally symmetric circulation in the wintertime troposphere, including a well-known model by *Palmén and Newton* [1969]. While resembling its original version proposed by *Rossby* [1941], it emphasizes more the concentration of westerly momentum into subtropical and polar-front jets and their respective association with the Hadley cell and a polar frontal zone. On the basis of the argument by *HV90* and our findings, a fundamental modification we would add to *Palmén's* model is the possible association among a polar-front jet, storm track, surface baroclinic zone over a subarctic frontal zone, as postulated in Figure 9a, which may add further significance to the midlatitude air–sea interaction. Unlike the polar frontal zone tilted distinctly poleward, a polar-front jet and associated baroclinic zone extend more vertically down to the surface just above the frontal zone (Figure 3). The jet is accompanied by a major storm track, and its deep structure is a manifestation of its eddy-driven nature [*Lee and Kim,* 2003].

Another point emphasized in Figure 9 is their distinct characteristics between the two types of jets, as a factor that influences the observed seasonal evolution of storm tracks. In fact, two types of schematics are presented in Figure 9 depending upon the strength of a subtropical jet, as in *Lee and Kim* [2003]. As speculated by *Palmén* [1951] and later elucidated theoretically [*Held and Hou,* 1980; *Lindzen and Hou*, 1988], the jet is formed through poleward transport of angular momentum by the Hadley cell, and the jet is much stronger in

the winter hemisphere where the Hadley cell is stronger. Zonal asymmetries in tropical SST distribution or the presence of a tropical landmass can lead to the localization of the jet [*Inatsu et al.,* 2002]. In fact, the formation of the SH subtropical jet is related to the Asian summer monsoon. Not driven by eddies, a subtropical jet may not necessarily accompany a distinct surface baroclinic zone. Indeed, the jet axis is between the subarctic and subtropical oceanic frontal zones over the North Pacific (Figure 6). Over the SH, the jet is located above a subtropical high-pressure belt, which is unfavorable for baroclinic eddy growth. Thus, a subtropical jet is shallow and confined around its tight core at the high tropopause, unless merged with a polar-front as in the wintertime North Pacific associated with a planetary-wave trough.

Through idealized numerical experiments, *Lee and Kim* [2003] examined how storm track activity depends on the subtropical jet intensity. They found that the main storm track forms along a polar-front jet, as in Figure 9a, only when a subtropical jet is weak, consistent with the observations [*NS02*, *NS04*]. However, the greatest discrepancy is that a subtropical jet, as it intensifies in the model, becomes increasingly favorable for baroclinic eddy growth. As opposed to their experiments, the jet intensification in the real atmosphere is unfavorable for storm track formation. Over each of the North and South Pacific, an intensified wintertime subtropical jet traps eddies into its core, keeping them away from a surface baroclinic zone anchored by a subarctic oceanic frontal zone. The trapping thus impairs eddy growth, despite the marked baroclinicity below the jet core. Over the South Pacific, where the two jets are well separated, the trapping leads to the meridional separation of the main storm track branch between the upper and lower levels [*NS04*]. We suggest this is a typical situation of the subtropical-jet-dominant regime (Figure 9b). No such separation occurs over the North Pacific, where the two jets are merged. Still, the subtropical jet traps eddy activity, resulting in the midwinter suppression of storm track activity. This is an intermediate situation between the two prototype situations in Figure 9. The storm track activity is enhanced in fall and spring when eddies can propagate above the subarctic frontal zone. This "weak subtropical-jet regime" (Figure 9a) appears more typically over the North Atlantic and the summertime SH. In the real atmosphere, the main storm track branch exhibits an apparent preference for staying with a polar-front jet, perhaps due to the anchoring effect by an underlying oceanic frontal zone. This preference may be underestimated in the idealized experiments by *Lee and Kim.* Their experiments would have been more realistic if well-defined surface baroclinic zones as observed had been prescribed.

Of course, the schematics in Figure 9 are nothing but a working hypothesis. Further observational and modeling study is hence needed to assess how relevant they are to extracting the essence of the atmospheric general circulation observed in the extratropics. More study is also needed to assess the robustness and detailed mechanisms of the positive feedback loop, if really exists, among a polar-front jet, storm track and subarctic frontal zone, and its importance in the climate variability. Especially, the significance of the anchoring effect by oceanic frontal zones should be confirmed in experiments with an AGCM with resolution high enough to resolve the cross-frontal thermal contrasts. It is also important to study how the oceanic fronts are maintained under the forcing from overlying storm tracks.

*Acknowledgments.* The authors thank Prof. S.-P. Xie for stimulating discussions and encouragement and Mr. Y. Onoue for preparing Figure 4. Comments by the two anonymous referees are greatly acknowledged. The Grid Analysis and Display System (GrADS) was used for drawing the figures.

## REFERENCES

Alexander, M. A., Midlatitude atmosphere–ocean interaction during El Niño, *J. Clim., 5*, 944–958, 1992.

Alexander, M. A., I. Bladé, M. Newman, J. R. Lanzante, N.-C. Lau, and J. D. Scott, The atmospheric bridge: The influence of ENSO teleconnection on air–sea interaction over the global oceans, *J. Clim., 15*, 2205–2231, 2002.

Alexander, M. A., N.-C. Lau, and J. D. Scott, Broadening the atmospheric bridge paradigm: ENSO teleconnections to the North Pacific in summer and to the tropical West Pacific–Indian Oceans over the seasonal cycle, 2004.

Bals-Elsholz, T. M., E. H. Atallah, L. F. Bosart, T. A. Wasula, M. J. Cempa, and A. R. Lupo, The wintertime Southern Hemisphere split jet: Structure, variability and evolution, *J. Clim., 14,* 4191–4215, 2001.

Barsugli, J. J., and D. S. Battisti, The basic effects of atmosphere–ocean thermal coupling on midlatitude variability, *J. Atmos. Sci., 55*, 477–493, 1998.

Berbery, E. H., and C. S. Vera, Characteristics of the Southern Hemisphere winter storm track with filtered and unfiltered data, *J. Atmos. Sci., 53*, 468–481, 1996.

Blackmon, M. L., J. M. Wallace, N.-C. Lau, and S. L. Mullen, An observational study of the Northern Hemisphere wintertime circulation, *J. Atmos. Sci., 34*, 1040–1053, 1977.

Blackmon, M. L., Y.-H. Lee, J. M. Wallace, and H.-H. Hsu, Time evolution of 500-mb height fluctuations with long, intermediate and short time scales as deduced from lag-correlation analysis, *J. Atmos. Sci., 41*, 981–991, 1984.

Bosart, L. F., Observed cyclone life cycles, *in The Life Cycles of Extratropical Cyclones,* edited by M. A. Shapiro and S. GrØnås, pp. 187–213, American Meteorological Society, Boston, MA, 1999.

Cai, M., Local instability dynamics of storm tracks, *in Observation, Theory and Modeling of Atmospheric Variability,* edited by X.

Zhu, X. Li, M. Cai, S. Zhou, Y. Zhu, F.-F. Jin, X. Zou and M. Zhang, pp. 3–38, World Scientific, Singapore, 2004.

Cayan, D. R., Latent and sensible heat-flux anomalies over the northern oceans – The connection to monthly atmospheric circulation, *J. Clim., 5*, 354–369, 1992a.

Cayan, D. R., Latent and sensible heat-flux anomalies over the northern oceans – Driving the sea–surface temperature, *J. Phys. Oceanogr., 22*, 859–881, 1992b.

Chang, E. K. M., Downstream development of baroclinic waves as inferred from regression analysis, *J. Atmos. Sci., 50*, 2038–2053, 1993.

Chang, E. K. M., Characteristics of wave packets in the upper troposphere. Part II: Seasonal and hemispheric variations, *J. Atmos. Sci., 56*, 1729–1747, 1999.

Chang, E. K. M., GCM and observational diagnoses of the seasonal and interannual variations of the Pacific storm track during the cool season, *J. Atmos. Sci., 58*, 1784–1800, 2001.

Chang, E. K. M., Midwinter suppression of the Pacific storm track activity as seen in aircraft observations, *J. Atmos. Sci., 60*, 1345–1358, 2003.

Chang, E. K. M., and D. B. Yu, Characteristics of wave packets in the upper troposphere. Part I: Northern Hemisphere winter, *J. Atmos. Sci., 56*, 1708–1728, 1999.

Chang, E. K. M., S. Lee, and K. L. Swanson, Storm track dynamics, *J. Clim., 15*, 2163–2183, 2002.

Charney, J. G., The dynamics of long waves in a baroclinic westerly current, *J. Meteorol., 4*, 135–163, 1947.

Chen, B., S. R. Smith, and D. H. Bromwich, Evolution of the tropospheric split jet over the South Pacific Ocean during the 1986–89 ENSO cycle, *Mon. Weather Rev., 124*, 1711–1731, 1996.

Christoph, M., U. Ulbrich, and P. Speth, Midwinter suppression of Northern Hemisphere storm track activity in the real atmosphere and in GCM experiments, *J. Atmos. Sci., 54,* 1589–1598, 1997.

Colling, A., *Ocean Circulation, 2nd Edition,* pp. 286, The Open University, Butterworth-Heinemann, Oxford, U.K., 2001.

Deser, C., and M. L. Blackmon, On the relationship between tropical and North Pacific sea–surface temperature variations, *J. Clim., 8*, 1677–1680, 1995.

Deser, C., and M. S. Timlin, Atmosphere–ocean interaction on weekly timescales in the North Atlantic and Pacific, *J. Clim., 10*, 393–408, 1997.

Dickson, R. R., and J. Namias, North American influences on the circulation and climate of the North Atlantic sector, *Mon. Weather Rev., 104,* 728–744, 1976.

Eady, E. T., Long waves and cyclone waves, *Tellus, 1*, 33–52, 1949.

Frankignoul, C., Sea surface temperature anomalies, planetary waves and air–sea feedback in the middle latitudes, *Rev. Geophys., 23*, 357–390 1985.

Frankignoul, C., and R. W. Reynolds, Testing a dynamical model for mid-latitude sea surface temperature anomalies, *J. Phys. Oceanogr., 13*, 1131–1145, 1983.

Gulev, G. K., T. Jung, and E. Ruprecht, Climatology and interannual variability in the intensity of synoptic-scale processes in the North Atlantic from the NCEP-NCAR reanalysis data, *J. Clim., 15*, 809–828 2003.

Halliwell, G. R., and D. A. Mayer, Frequency response properties of forced climatic SST anomaly variability in the North Atlantic, *J. Clim., 9*, 3575–3587, 1996.

Hanawa, K., R. Sannomiya, and Y. Tanimoto, Static relationship between anomalies of SSTs and air–sea heat fluxes in the North Pacific, *J. Meteorol. Soc. Jpn., 73*, 757–763, 1995.

Held, I. M., Planetary waves and their interaction with smaller scales, *in The Life Cycles of Extratropical Cyclones,* edited by M. A. Shapiro and S. GrØnås, pp. 101–109, American Meteorological Society, Boston, MA, 1999.

Held, I. M., and A. Y. Hou, Nonlinear axially symmetric circulations in a nearly inviscid atmosphere, *J. Atmos. Sci.,* 37, 515–533, 1980.

Hoerling, M. P., and M. Ting, On the organization of extratropical transients during El Niño, *J. Clim., 7*, 745–766, 1994.

Hoerling, M. P., and A. Kumar, Atmospheric response patterns associated with tropical forcing, *J. Clim., 15*, 2184–2203, 2002.

Hoskins, B. J., and P. J. Valdes, On the existence of storm tracks, *J. Atmos. Sci., 47*, 1854–1864, 1990.

Hoskins, B. J., and K. I. Hodges, New perspectives on the Northern Hemisphere winter storm tracks, *J. Atmos. Sci., 59*, 1041–1061, 2002.

Hoskins, B. J., M. E. McIntyre, and A. W. Robertson, On the use and significance of isentropic potential vorticity maps, *Q. J. R. Meteorol. Soc., 111*, 877–946, 1985.

Inatsu, M., H. Mukougawa, and S.-P. Xie, Atmospheric response to zonal variations in mid-latitude SST: Transient and stationary eddies and their feedback, *J. Clim.*, *16*, 3314–3329, 2003.

Karoly, D. J., D. G. Vincent, and J. M. Schrage, General circulation, *in Meteorology of the Southern Hemisphere, Meteorol. Monogr., 49*, edited by D. J. Karoly and D. G. Vincent, pp. 47–86, American Meteorological Society, Boston, MA, 1998.

Kelly, K. A., and S. Dong, The relationship of western boundary current heat transport and storage to mid-latitude ocean–atmosphere interaction, 2004.

Klein, W. H., The frequency of cyclones and anticyclones in relation to the mean circulation, *J. Meteorol., 15*, 98–102, 1958.

Kuo, Y.-H., R. J. Reed, and S. Low-Nam, Effects of surface energy fluxes during the early development and rapid intensification stages of seven explosive cyclones in the western Atlantic, *Mon. Weather Rev., 119*, 457–476, 1991.

Kushnir, Y., W. A. Robinson, I. Bladé, N. M. J. Hall, S. Peng, and R. Sutton, Atmospheric GCM response to extratropical SST anomalies: Synthesis and evaluation, *J. Clim., 15*, 2233–2256, 2002.

Lau, N.-C., Interactions between global SST anomalies and the midlatitude atmospheric circulation, *Bull. Am. Meteorol. Soc., 78*, 21–33, 1997.

Lau, N.-C., and E. O. Holopainen, Transient eddy forcing of the time-mean flow as identified by quasi-geostrophic tendencies, *J. Atmos. Sci., 41*, 313–328, 1984.

Lau, N.-C., and M. J. Nath, A modeling study of the relative roles of the tropical and extra-tropical SST anomalies in the variability of the global atmosphere–ocean system, *J. Clim., 7*, 1184–1207, 1994.

Lau, N.-C., and M. J. Nath, The role of the "atmospheric bridge" in linking the tropical Pacific ENSO events to extratropical SST anomalies, *J. Clim., 9*, 2036–2057, 1996.

Lau, N.-C., and M. J. Nath, Impact of ENSO on SST variability in

the North Pacific and North Atlantic: Seasonal dependence and role of extratropical air–sea coupling, *J. Clim., 14*, 2846–2866, 2001.

Lee, S., and I. M. Held, Baroclinic wave packets in models and observations, *J. Atmos. Sci., 50*, 1413–1428, 1993.

Lee, S., and H.-K. Kim, The dynamical relationship between subtropical and eddy-driven jets, *J. Atmos. Sci., 60*, 1490–1503, 2003.

Lindzen, R. S., and A. Y. Hou, Hadley circulations for zonally averaged heating centered off the equator, *J. Atmos. Sci., 45*, 2416–2427, 1998.

Lukas, R. B., Freshening of the upper pycnocline in the North Pacific subtropical gyre associated with decadal changes of rainfall, *Geophys. Res. Lett., 28*, 3485–3488, 2001.

Miller, A. J., D. R Cayan, T. P. Barnett, N. E. Graham, and J. M. Oberhuber, Interdecadal variability of the Pacific Ocean: Model response to observed heat flux and wind stress anomalies, *Clim. Dyn., 9*, 287–302, 1994.

Mohri, K., On the fields of wind and temperature over Japan and adjacent waters during winter of 1950–1951, *Tellus, 3*, 340–358, 1953.

Nagasawa, M., Y. Niwa, and T. Hibiya, Spatial and temporal distribution of the wind-induced internal wave energy available for deep water mixing in the North Pacific, *J. Geophys. Res., 105*, 13,933–13,943, 2000.

Nakamura, H., Midwinter suppression of baroclinic wave activity in the Pacific, *J. Atmos. Sci., 49*, 1629–1641, 1992.

Nakamura, H., and T. Yamagata, Recent decadal SST variability in the Northwestern Pacific and associated atmospheric anomalies, *in Beyond El Niño: Decadal and Interdecadal Climate Variability*, edited by A. Navarra, pp. 49–72, Springer-Verlag, Berlin, Germany, 1999.

Nakamura, H., and T. Sampe, Trapping of synoptic-scale disturbances into the North-Pacific subtropical jet core, *Geophys. Res. Lett., 29*, doi:1029/2002GL015335, 2002.

Nakamura, H., and A. S. Kazmin, Decadal changes in the North Pacific oceanic frontal zones as revealed in ship and satellite observations, *J. Geophys. Res., 108*, doi:10.1029/ JC19990085, 2003.

Nakamura, H., and A. Shimpo, Seasonal variations in the Southern Hemisphere storm tracks and jet streams as revealed in a reanalysis data set, *J. Clim., 17*, 1828–1842, 2004.

Nakamura, H., G. Lin, and T. Yamagata, Decadal climate variability in the North Pacific during the recent decades, *Bull. Am. Meteorol. Soc., 78*, 2215–2225, 1997a.

Nakamura, H., M. Nakamura, and J. L. Anderson, The role of high- and low-frequency dynamics in blocking formation, *Mon. Weather Rev., 125,* 2074–2093, 1997b.

Nakamura, H., T. Izumi, and T. Sampe, Interannual and decadal modulations recently observed in the Pacific storm track activity and East Asian winter monsoon, *J. Clim., 15*, 1855–1874, 2002.

Namias, J., and D. R. Cayan, Large-scale air–sea interactions and short period climate fluctuations, *Science, 214*, 869–874, 1981.

Neiman, P. J., and M. A. Shapiro, The life cycle of an extratropical marine cyclone. Part I: Frontal cyclone evolution and thermodynamic air–sea interaction, *Mon. Weather Rev., 121*, 2153–2176, 1993.

Nitta, T., and S. Yamada, Recent warming of tropical sea surface temperature and its relationship to the northern hemisphere circulation, *J. Meteorol. Soc. Jpn.*, *67*, 375–383, 1989.

Nonaka, M., and S.-P. Xie, Co-variations of sea surface temperature and wind over the Kuroshio and its extension: Evidence for ocean-to-atmospheric feedback, *J. Clim.*, *16*, 1404–1413, 2003.

Nuss, W. A., and S. I. Kamikawa, Dynamics and boundary layer processes in two Asian cyclones, *Mon. Weather Rev., 118*, 755–771, 1990.

Oberhuber, J. M., The Budget of Heat, Buoyancy and Turbulent Kinetic Energy at the Surface of the Global Ocean*, Rep. 15*, 19 pp., Max Plank Institut für Meteolorogie, Hamburg, Germany, 1988.

Orlanski, I., and E. K. M. Chang, Ageostrophic geopotential fluxes in downstream and upstream development of baroclinic waves, *J. Atmos. Sci., 50*, 212–225, 1993.

Palmén, E., The role of atmospheric disturbances in the general circulation, *Q. J. R. Meteorol. Soc., 77*, 337–354, 1951.

Palmén, E., and C. W. Newton, *Atmospheric Circulation Systems: Their Structure and Physical Interpretation,* 603 pp., Academic Press, New York, N.Y., 1969.

Peng, S., and J. S. Whitaker, Mechanisms determining the atmospheric response to midlatitude SST anomalies, *J. Clim., 12*, 1393–1408, 1999.

Peng, S., and W. A. Robinson, Relationships between atmospheric internal variability and the responses to an extra-tropical SST anomaly, *J. Clim., 14*, 2943–2959, 2001.

Petterssen, S., *Weather and Forecasting, 2nd Edition, Vol. 1*, 428 pp., McGraw Hill, New York, N.Y., 1956.

Petterssen, S., and S. J. Smebye, On the development of extra-tropical cyclones, *Q. J. R. Meteorol. Soc., 97*, 457–482, 1971.

Qiu, B., Interannual variability of the Kuroshio Extension system and its impact on their wintertime SST field*, J. Phys. Oceanogr., 30*, 1486–1502, 2000.

Qiu, B., The Kuroshio extension system: Its large-scale variability and role in the midlatitude ocean–atmosphere interaction, *J. Oceanogr., 58*, 57–75, 2002.

Qiu, B., Kuroshio Extension variability and forcing of the Pacific decadal oscillations: Responses and potential feedback, *J. Phys. Oceanogr.*, *33*, 2465–2482, 2003.

Qiu, B., and K.A. Kelly, Upper-ocean heat balance in the Kuro-shio extension region, *J. Phys. Oceanogr., 23*, 2027–2041, 1993.

Randel, W. J., and P. A. Newman, The stratosphere in the Southern Hemisphere, *in Meteorology of the Southern Hemisphere, Meteorol. Monogr., 49,* edited by D. J. Karoly and D. G. Vincent, pp. 243–282, American Meteorological Society, Boston, M.A., 1998.

Rao, V. B., A. M. C. do Carmo, and S. H. Franchito, Seasonal variations in the Southern Hemisphere storm tracks and wave propagation, *J. Atmos. Sci., 59*, 1029–1040, 2002.

Reed, R. J., G. A. Grell, and Y.-H. Kuo, The ERICA IOP-5 Storm: Part I: Analysis and simulation, *Mon. Weather Rev., 121*, 1577–1594, 1993.

Reynolds, R. W., and T. M. Smith, Improved global sea surface temperature analysis using optimum interpolation, *J. Clim., 7*, 929–948, 1994.

Rogers, J. C., Patterns of low-frequency monthly sea level pressure variability (1899–1986) and associated wave cyclone frequencies, *J. Clim., 3*, 1364–1379, 1990.

Rossby, C.-G., The scientific basis of modern meteorology, *in Yearbook of Agriculture, Climate and Man,* edited by G. Hambidge, pp. 599–655, U.S. Government Printing Office, Washington, D.C., 1941.

Sanders, F., and J. R. Gyakum, Synoptic-dynamic climatology of the "bomb", *Mon. Weather Rev., 108*, 1589–1606, 1980.

Schneider, N., A. J. Miller and D. W. Pierce, Anatomy of North Pacific decadal variability, *J. Clim.*, *15*, 586–605, 2002.

Seager, R., Y. Kushnir, M. Visbeck, N. Naik, J. Miller, G. Krahmann, and H. Cullen, Causes of Atlantic Ocean climate variability between 1958 and 1998, *J. Clim.*, *13*, 2845–2862, 2000.

Seager, R., A. Karspeck, M. Cane, Y. Kushnir, A. Giannini, A. Kaplan, B. Kerman, and J. Miller, Predicting Pacific decadal variability, 2004.

Simmonds, I., and K. Keay, Mean Southern Hemisphere extratropical behavior in the 40-year NCEP-NCAR reanalysis *J. Clim., 13*, 873–885, 2000.

Simmons, A. J., J. M. Wallace, and G. W. Branstator, Barotropic wave propagation and instability, and atmospheric teleconnection patterns, *J. Atmos. Sci., 40*, 1363–1392, 1983.

Sinclair, M. R., An objective cyclone climatology for the Southern Hemisphere, *Mon. Weather Rev., 122*, 2239–2256, 1994.

Sinclair, M. R., A climatology of cyclogenesis for the Southern Hemisphere, *Mon. Weather Rev., 123*, 1601–1619, 1995.

Swanson, K. L., and R. T. Pierrehumbert, Nonlinear wave packet evolution on a baroclinically unstable jet, *J. Atmos. Sci., 51*, 384–396 1994.

Takaya, K., and H. Nakamura, A formulation of a phase-independent wave-activity flux for stationary and migratory quasi-geostrophic eddies on a zonally varying basic flow, *J. Atmos. Sci., 58*, 608–627, 2001.

Takayabu, I., "Coupling development": An efficient mechanism of the development of extratropical cyclones, *J. Meteorol. Soc. Jpn., 69*, 609–628, 1991.

Tanimoto, Y., N. Iwasaka, and K. Hanawa, Relationship between sea surface temperature, the atmospheric circulation and air–sea fluxes on multiple time scales, *J. Meteorol. Soc. Jpn., 75*, 831–849, 1997.

Tanimoto, Y., H. Nakamura, T. Kagimoto, and S. Yamane, An active role of extratropical sea surface temperature anomalies in determining anomalous turbulent heat fluxes, *J. Geophys. Res., 108*, 3304, doi:10.1029/2002JC00175, 2003.

Tomita, T., B. Wang, T. Yasunari, and H. Nakamura, Global patterns of decadal-scale variability observed in sea surface temperature and lower-tropospheric circulation fields, *J. Geophys. Res.*, *106*, 26,805–26,815, 2001.

Tomita, T., S.-P. Xie, and M. Nonaka, Estimates of surface and subsurface forcing for decadal sea surface temperature variability in the mid-latitude North Pacific, *J. Meteorol. Soc. Jpn., 79*, 1289–1300, 2002.

Trenberth, K. E., An assessment of the impact of transient eddies on the zonal flow during a blocking episode using localized Eliassen-Palm flux diagnosis, *J. Atmos. Sci., 43*, 2070–2087, 1986.

Trenberth, K. E., Storm tracks in the Southern Hemisphere, *J. Atmos. Sci., 48*, 2159–2178, 1991.

Trenberth, K. E., W. G. Large, and J. G. Olson, The mean annual cycle in global ocean wind stress, *J. Phys. Oceanogr., 20*, 1742–1760, 1990.

Wallace, J. M., and D. S. Gutzler, Teleconnections in the geopotential height field during the Northern Hemisphere winter, *Mon. Weather Rev*., *109*, 784–812, 1981.

Wallace, J. M., and Q.-R. Jiang, On the observed structure of interannual variability of the atmosphere/ocean climate system, *in Atmosphere and Oceanic Variability,* edited by H. Cattle, pp. 17–43, Royal Meteorological Society, Reading, U.K., 1987.

Wallace, J. M., G.-H. Lim, and M. L. Blackmon, Relationship between cyclone tracks, anticyclone tracks and baroclinic waveguides, *J. Atmos. Sci., 45*, 439–462, 1988.

Watanabe, M., and M. Kimoto, Atmosphere–ocean thermal coupling in the North Atlantic: A positive feedback, *Q. J. R. Meteorol. Soc., 126*, 3343–3369, 2000.

Whittaker, L. M., and L. H. Horn, Northern Hemisphere extra-tropical cyclone activity for four mid-season months, *Int. J. Climatol., 4*, 297–310, 1984.

Xie, S.-P., Satellite observations of cool ocean–atmosphere interaction, *Bull. Am. Meteorol. Soc., 85*, 195–208, 2004.

Xie, S.-P., T. Kunitani, A. Kubokawa, M. Nonaka and S. Hosoda, Interdecadal thermocline variability in the North Pacific for 1958–1997: A GCM simulation, *J. Phys. Oceanogr.*, *30*, 2798–2813, 2000.

Xie, S.-P., J. Hafner, Y. Tanimoto, W. T. Liu, H. Tokinaga, and H. Xu, Bathymetric effect on the winter sea surface temperature and climate of the Yellow and East China Seas, *Geophys. Res. Lett.*, *29*, 3261, doi:10.1029/2002GL015884, 2002.

Yasuda, I., K. Okuda, and Y. Shimizu, Distribution and modification of North Pacific intermediate water in the Kuroshio-Oyashio Interfrontal Zone, *J. Phys. Oceanogr., 26*, 448–465, 1996.

Yuan, X., and L. D. Talley, The subarctic frontal zone in the North Pacific: Characteristics of frontal structure from climatological data and synoptic surveys, *J. Geophys. Res., 101*, 16,491–16,508, 1996.

Zhang, Y., and I. M. Held, A linear stochastic model of a GCM's midlatitude storm tracks, *J. Atmos. Sci., 56,* 3416–3435, 1999.

---

H. Nakamura and T. Sampe, Department of Earth and Planetary Science, University of Tokyo, Tokyo, 113–0033, Japan. (hisashi@eps.s.u-tokyo.ac.jp; sampe@eps.s.u-tokyo.ac.jp)

A. Shimpo, Climate Prediction Division, Marine and Climate Department, Japan Meteorological Agency, Tokyo, 100–0004, Japan. (sinpo@naps.kishou.go.jp)

Y. Tanimoto, Graduate School of Environmental Earth Science, Hokkaido University, Sapporo, 060–0810, Japan. (tanimoto@ees.hokudai.ac.jp)